Homogenous and multilayer electromagnetics models for estimating skin reflectance

Amani Yousef Owda[1], Majdi Owda[2]
[1]Department of Natural, Engineering and Technology Sciences, Faculty of Graduate Studies, Arab American University, Jenin, Palestine
[2]Faculty of Data Science, UNESCO Chair on Data Science for Sustainable Development, Arab American University, Jenin, Palestine

Article Info	ABSTRACT

Reflectance measurements of human skin are widely limited over the millimeter wave (MMW) band in literature. This is due to the cost and technical difficulties of the experimental setup. This paper proposes homogenous and multilayer skin models for estimating the reflectance of the forearm and palm of the hand skin over the MMW band 30-100 GHz. The simulation results demonstrate that the differences in reflectance between the homogenous and multilayer models of forearm skin are limited to 0.014, indicating that the thin stratum corneum (SC) layer in the multilayer skin models has a minimal impact on the interaction with MMW of the forearm skin. However, in the palm of hand skin, there is a substantial difference in reflectance calculations between the homogenous and the multilayer skin models in the range of 0.099 to 0.143. These differences are attributed to the presence of a thick SC layer in the palm of the hand. Thus, the simulation results suggested that two-layer should be used for the palm of hand skin as it better captures the reflectance characteristics of this region. The importance of having those models are in calculating the skin reflectance that can be used for the non-invasive diagnosis of skin conditions.

Corresponding Author:

Amani Yousef Owda
Department of Natural, Engineering and Technology Sciences, Faculty of Graduate Studies
Arab American University
P600, Ramallah, Palestine
Email: amani.owda@aaup.edu

1. INTRODUCTION

The electromagnetic spectrum's millimeter-wave (MMW) is an area of radio waves ranging from 30 GHz to 300 GHz [1], [2]. Signatures of the skin in the MMW band were measured in two ways: active sensing [3]–[5], which involves exposing the target area of the skin to non-ionizing radiation [6], [7], and passive sensing technology [8], [9], which does not involve exposure to any form of artificial radiation. Active sensing uses MMW radiation to measure the skin reflectance and signature, while passive sensing collects MMW emission to quantify the reflectance of the skin [10].

MMW frequency band offers potential for novel medical applications such as body sensing [11], [12], non-invasive diagnoses of skin diseases [8], [13], [14], and early detection of skin cancer [15]. Researchers' findings in [3], [4], [16], [17] suggest that significant variations in the dielectric properties and reflectivity of the skin exist between different locations. This can be attributed to variation in water content, as skin with higher water content tends to have higher reflectivity and lower dielectric properties than skin with lower water content [18]. To measure the reflectance and dielectric properties of the skin, the researchers in [3], [4], [16] used open-ended coaxial probes. This approach has been used widely in the literature to measure the reflectivity and the skin properties such as the relative complex permittivity. Experimental measurements obtained in [19]

showed a well define contrast in reflectance between healthy skin and skin with basal cell carcinoma (BCC). These results identified the tumor's boundaries, and this helping out the healthcare professional to identify the margin of the BCC accurately. This provides a more accurate treatment of BCC. Researchers in [4], [18] found that wet skin i.e. (skin after adding water) has higher dielectric properties and reflectance compared with normal skin. These results are consistent with the other studies conducted on normal and wet skin in [5], [20] and indicated that increasing the water content makes the skin more reflective. Reflectance measurements applied on ex vivo porcine skin samples in [21] indicated that the reflectance of burn-damaged skin was lower than that of normal skin. These differences in signatures between healthy and burn-damaged skin are due to lower water content in burn-damaged skin. These results prove that water content has a clear impact on the reflectance of the skin.

Although coaxial probes have been used widely in literature for the non-invasive diagnosis of skin diseases, there are many challenges and limitations for the use of the probe that can be addressed as follows: i) the probes are very sensitive to alignments and thus making it difficult to get accurate measurements as well as difficulty in calibrating the probes. ii) It is required to maintain constant pressure on the target area of the skin to get accurate and precise measurements [4], [22]. iii) The probes must be allocated in direct contact with the skin region and this makes it difficult to perform reflectance measurements on diseased skin such as burns and cancer [4], [22]. Figure 1 illustrates the use of the coaxial probe for measuring the dielectric properties of the human skin.
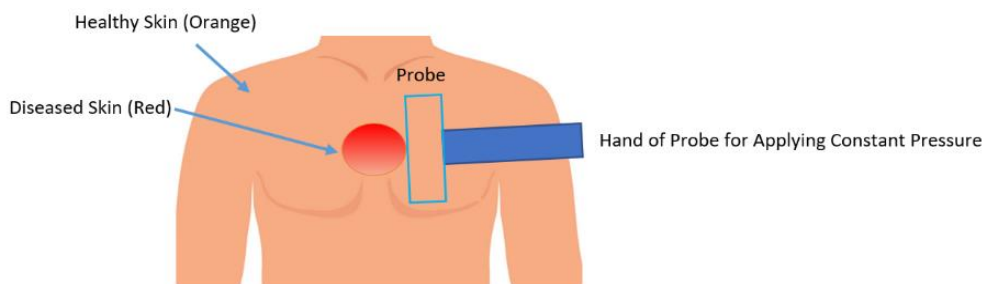

Figure 1. Open-ended coaxial probe for measuring the dielectric permittivity

Radiometry as a passive and a non-contact sensor has been suggested to measure the reflectance and the emissivity of healthy and diseased skin in the MMW region [23] as illustrated in Figure 2. The study conducted in [12] indicated substantial differences in the reflectance between normal and burn-damaged skin, and these differences are found to be increased with the degree of the burn. This indicates the potential of using radiometry in the non-invasive diagnosis of diseased skin. Similarly, the study in [23] demonstrated for the first time the use of radiometry as a non-contact sensor for the early detection of skin diseases and disorders in tens of seconds and without the need of being in a healthcare clinic. The radiometric measurements in this study [23] were performed on healthy skin and non-healthy skin having burns, melanoma skin cancers, and eczema. Experimental results in [23] demonstrate the potential of using radiometry for detecting skin diseases and conditions. The study proposed in [24] indicates that the reflectivity of the skin at 45 GHz can provide a better assessment of diabetic neuropathy. Das *et al.* [25] proposes a simulation approach for estimating the absorption of the skin using the reflectance database. Monte Carlo simulation in [26] was used to assess the interaction of clothing with the skin at 60 GHz. The skin models in [27] were used for presenting the complex tissue structures of the skin.
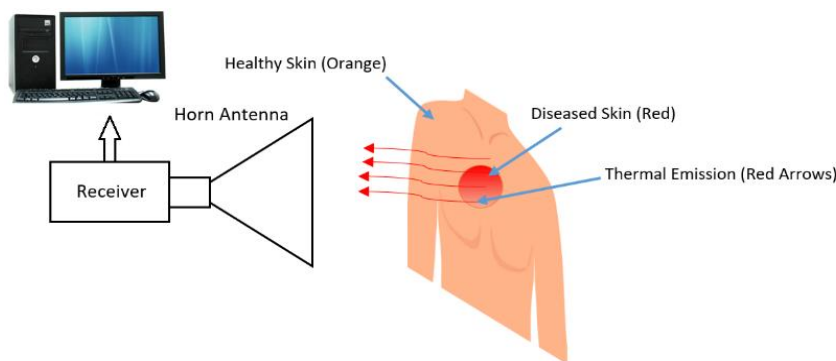

Figure 2. Radiomerter measuring the skin reflectance

In the literature review, comprehensive research has been done to investigate the feasibility of MMW technology in the non-invasive diagnosis of skin diseases using reflectivity and dielectric properties measurements as summarized in Table 1. The main limitation of active sensing techniques is that they are incredibly expensive, as the devices are available over specific frequency bands, and changing the frequency band is required to change the devices to fit the frequency band and this needs significant financial resources. Not only is the initial cost high but maintenance can also be costly. Furthermore, depending on the frequency band in use, it may require a new device each time the frequency band is changed, which can add up quickly. As a result, these techniques can be a major financial burden as well as technical difficulties and complexity in conducting the measurements. As an alternative, this paper proposed electromagnetics models of the forearm (thin skin) and palm of the hand (thick skin) that can be used for estimating the reflectance of the skin in the whole MMW band.

Table 1. Methods used for measuring skin reflectance in the MMW band

Frequency (GHz)	Method used	Skin type	References
30-40	Open-ended probe	Healthy skin	[4]
		Dry and wet	
		Burn damaged skin	
37-74	Open-ended probe	Healthy skin	[20], [28]
30-100	Open-ended probe	Healthy skin	[22]
30-60	Coaxial slim probe	Healthy skin	[29]
30-60	Waveguide	Healthy skin	[30]
57-100	Free space method	Dry and wet skin	[5]
90-100	Free space method	Dry and wet skin	[5]

This paper proposes single and multilayer electromagnetics models of the forearm and palm of the hand skin. The models extracted reflectance of the skin over a wide range of frequencies (30 GHz to 100 GHz) using the dielectric permittivity of the skin that can be obtained directly from the debye equation described in section 2 (19). The proposed models herein can estimate the reflectivity of the skin automatically by converting the dielectric permittivity to reflectivity without the need of involving the human subject. Moreover, the models reveal that the interaction of MMW doesn't go beyond the dermis layer of the skin. This is due to the low penetration of the millimeter wave radiation in the human skin as a result of the attenuation effect that is caused by the water content. This makes MMW frequency band suitable for assessing skin diseases and conditions.

2. METHOD

This section provides details about the main methodology used for building the skin models as illustrated in Figure 3. The first step is data collection in which the dielectric properties of the forearm and palm of hand skin were collected from different resources in the literature [20], [28], [31]. The second step is building different electromagnetics models for the forearm and palm of hand skin namely: i) a homogenous model, ii) a two-layer model, and iii) a three-layer model. The third step is model validation in which the calculated reflectance from the three models was compared with reflectance measurements conducted in the literature. Finally, featured applications of the skin models are introduced in the area of medical applications to distinguish between non-healthy and healthy skin.
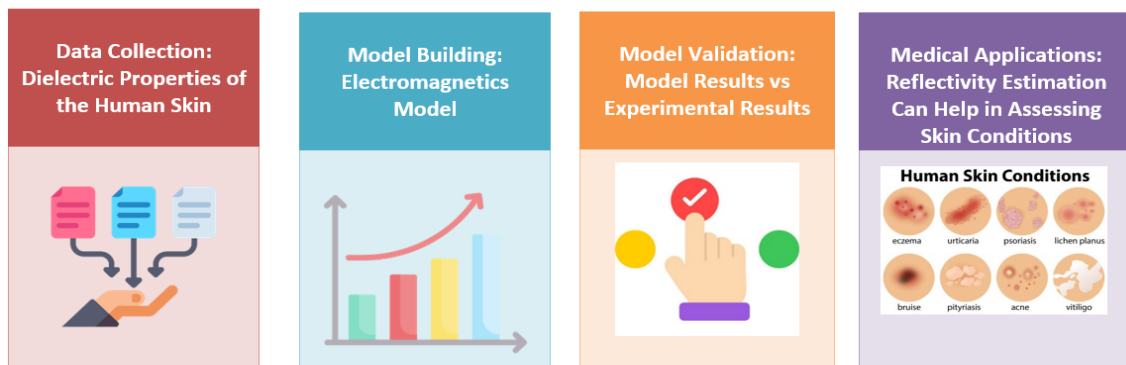

Figure 3. Methodology used in developing the forearm and the palm of the hand models

2.1. Mutilayer electromagnetics model

In this paper, the multilayer electromagnetic model is constructed and developed to calculate the reflectance of the palm of hand skin and forearm skin. Each layer of the model is characterized by three parameters; permittivity (ϵ), permeability (μ) and thickness of the layer (h). The first and the last layer of the model are semi-infinite. The structure of the multilayer electromagnetic model is presented as illustrated in Figure 4.
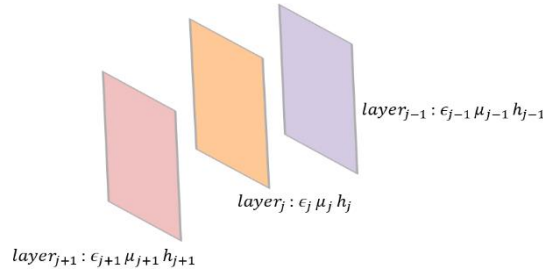

Figure 4. Multilayer electromagnetic model; each layer of the model is characterized by three parameters and those are permittivity (ϵ), permeability (μ) and thickness of the layer (h)

The permittivity of the skin ϵ is described in (1). It is a complex quantity that is consisted of two terms, namely: the free space permittivity, ϵ_o = 8.85 x 10^-12 F/m and the relative complex permittivity, ϵ_r. The relative complex permittivity ϵ_r is described in (2). The real part of the complex permittivity, ϵ'_r represents the dielectric constant of the skin. Whereas, the imaginary part of the complex permittivity, ϵ''_r represents the loss factor of the skin, ω is the angular frequency, and σ is the conductivity of the skin.

$$\epsilon = \epsilon_o \epsilon_r \tag{1}$$

$$\epsilon_r = \epsilon'_r - j\epsilon''_r = \epsilon\left[1 - \frac{j\sigma}{\omega\epsilon}\right] \tag{2}$$

The S-polarized plane wave propagating in the j-1 layer of an n-layer structure is presented in (3) and (4). The wave vector, kj is described in (5). Whereas, the wave number in free space, k_0 is expressed in (6). The speed of the light, c is equal $3x10^8 m/s$ and θ is the angle of incidence in the semi-infinite incident medium. In (3) and (4) can be expressed in a matrix format as illustrated in (7). For simplification, the recursion relation can be written as illustrated in (8) and (9).

$$\tilde{E}_{0+j-1} = 0.5\left(1 + \frac{\mu_{j-1}k_j}{\mu_j k_{j-1}}\right)e^{(-ik_{j-1}h_{j-1})}\tilde{E}_{0+j} + 0.5\left(1 - \frac{\mu_{j-1}k_j}{\mu_j k_{j-1}}\right)e^{(-ik_{j-1}h_{j-1})}\tilde{E}_{0-j} \tag{3}$$

$$\tilde{E}_{0-j-1} = 0.5\left(1 - \frac{\mu_{j-1}k_j}{\mu_j k_{j-1}}\right)e^{(ik_{j-1}h_{j-1})}\tilde{E}_{0+j} + 0.5\left(1 + \frac{\mu_{j-1}k_j}{\mu_j k_{j-1}}\right)e^{(ik_{j-1}h_{j-1})}\tilde{E}_{0-j} \tag{4}$$

$$k_j = k_0\sqrt{\epsilon_j\mu_j - \epsilon_1\mu_1 sin^2(\theta)} \tag{5}$$

$$k_0 = \frac{\omega}{c} \tag{6}$$

$$E_{j-1} = \begin{bmatrix} 0.5\left(1 + \frac{\mu_{j-1}k_j}{\mu_j k_{j-1}}\right)e^{(-ik_{j-1}h_{j-1})} & 0.5\left(1 - \frac{\mu_{j-1}k_j}{\mu_j k_{j-1}}\right)e^{(-ik_{j-1}h_{j-1})} \\ 0.5\left(1 - \frac{\mu_{j-1}k_j}{\mu_j k_{j-1}}\right)e^{(ik_{j-1}h_{j-1})} & 0.5\left(1 + \frac{\mu_{j-1}k_j}{\mu_j k_{j-1}}\right)e^{(ik_{j-1}h_{j-1})} \end{bmatrix}\begin{bmatrix}\tilde{E}_{0+j} \\ \tilde{E}_{0-j}\end{bmatrix} \tag{7}$$

$$E_1 = M_2 \dots M_{j-1}M_j E_j \tag{8}$$

$$E_1 = M_2 \dots M_{j-1}M_n E_n \tag{9}$$

In (8) and (9) can be written in a matrix format for *j* and *n-layer* as illustrated in (10). G$_j$ and G_n in (10) are 2×2 matrix presented in (11). The two components of the electric field $\tilde{E}_{0+1}$ and $\tilde{E}_{0-1}$ are presented

in (12) and (13). Since there is no reflected wave in the nth layer, replace $g_{n1,2}\tilde{E}_{0-n}$ and $g_{n2,2}\tilde{E}_{0-n}$ with zero in (12) and (13). This simplify the equations as illustrated in (14) and (15).

$$E_1 = G_j E_j \text{ and } E_1 = G_n E_n \tag{10}$$

$$G_j = \begin{bmatrix} g_{j1,1} & g_{j1,2} \\ g_{j2,1} & g_{j2,2} \end{bmatrix} \text{ and } G_n = \begin{bmatrix} g_{n1,1} & g_{n1,2} \\ g_{n2,1} & g_{n2,2} \end{bmatrix} \tag{11}$$

$$\tilde{E}_{0+1} = g_{n1,1}\tilde{E}_{0+n} + g_{n1,2}\tilde{E}_{0-n} \tag{12}$$

$$\tilde{E}_{0-1} = g_{n2,1}\tilde{E}_{0+n} + g_{n2,2}\tilde{E}_{0-n} \tag{13}$$

$$\tilde{E}_{0+1} = g_{n1,1}\tilde{E}_{0+n} \tag{14}$$

$$\tilde{E}_{0-1} = g_{n2,1}\tilde{E}_{0+n} \tag{15}$$

From (14) and (15), reflectivity Γ and transmissivity τ can be expressed as illustrated in (16) and (17). The application of conservation of energy, results in the relationship between the reflectance $R = |\Gamma|^2$, and transmittance $T = |\tau|^2$ from the skin's as shown in (18). The relative complex permittivity is required for reflectance calculations. The data of the relative complex permittivity for each model are calculated from debye equation i.e. (19) and the parameters of the equation are obtained from [20], [28], [31]. In (19); $i = \sqrt{-1}$, ϵ_s and ϵ_∞ present the relative permittivity below and above the relaxation frequency respectively, σ_s is the static conductivity and τ is the central relaxation time.

$$\Gamma = \frac{\tilde{E}_{0-1}}{\tilde{E}_{0+1}} = \frac{g_{n2,1}}{g_{n1,1}} \tag{16}$$

$$\tau = \frac{\tilde{E}_{0+n}}{\tilde{E}_{0+1}} = \frac{1}{g_{n1,1}} \tag{17}$$

$$R + T = 1 \tag{18}$$

$$\epsilon_r = \epsilon_\infty + \frac{\epsilon_s - \epsilon_\infty}{1 + \omega\tau} - i\frac{\sigma_s}{\omega\epsilon_o} \tag{19}$$

Based on (3)-(18); the three models of the skin were developed to calculate the reflectance of the forearm and palm of hand skin. The relative complex permittivity is required for reflectance calculations. The data of the relative complex permittivity for each model of the skin are calculated using debye equation with single relaxation time [16], [31], [32]. Figure 5 shows the structure of the three models of the skin and those are: i) homogenous unilayer skin model, ii) two-layer skin model, and iii) three-layer skin model. In the homogenous unilayer model in Figure 5(a), the skin is assumed to have a single homogenous semi-infinite layer. In the two-layer model illustrated in Figure 5(b), the skin is assumed to have two layers and those are: i) finite thickness stratum corneum (SC) layer and ii) semi-infinite epidermis plus dermis layer. In the three-layer model in Figure 5(c), the skin is assumed to have three layers namely: i) finite thickness stratum corneum layer, ii) finite thickness epidermis plus dermis layer, and iii) semi-infinite fat layer. The thickness of each layer of the skin in multilayered models is specified as illustrated in Table 2. The thicknesses of skin layers in Table 2, show that the palm of hand skin is thicker than the forearm skin.
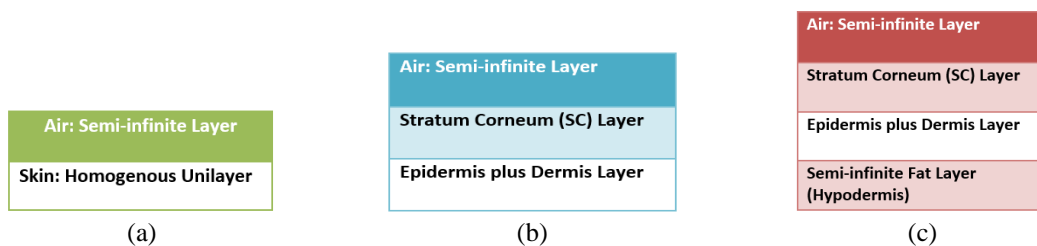

Figure 5. Homogenous and multilayer models used for estimating the reflectance of forearm and palm of hand skin; (a) homogenous model, (b) two-layer model, and (c) three-layer model

Table 2. Thicknesses of skin layers used in multilayer models of forearm and palm of hand skin

Region	Two-layer	Three-layer
Forearm skin	SC thickness: 0.015 mm [20], [28]	SC thickness: 0.015 mm Epidermis plus Dermis thickness: 1.45 mm [20], [28]
Palm of hand skin	SC thickness: 0.43 mm [20]	SC thickness: 0.43 mm Epidermis plus Dermis thickness: 1.85 mm [20]

3. RESULTS AND DISCUSSION

Reflectance of the palm of hand and the forearm skin obtained from the homogenous model, two-layer model and three-layer model are presented and discussed in the following sections: i) section 3.1 presents reflectance of palm of hand skin, ii) section 3.2 presents reflectance for forearm skin, iii) section 3.3 presents models validation, and iv) section 3.4 shows featured application of the proposed models.

3.1. Reflectance of Palm of Hand

This secton presents the reflectance of palm of hand skin obtained from the three models described in section 2. The reflectance of palm of hand skin is calculated over the frequency band 30-100 GHz using the three models as illustrated in Figure 6. Three models were used namely: i) homogenous skin model Figure 6(a), ii) two-layer skin model Figure 6(b), and iii) three-layer skin model Figure 6(c). Reflectance results in Figure 6 indicate differences in reflectance values obtained from homogenous skin model as in Figure 6(a) and multilayer skin models as in Figures 6(b)-6(c). Results in Figure 6(d) show that the differences in reflectance between the homogenous and multilayer skin models is substantial and it is varied in the range of 0.099 to 0.143 over the frequency band 30-100 GHz. The presence of thick SC layer in the two and the three-layer skin models makes the difference in reflectance substantial due to the significant interaction of the thick SC layer with the MMW [20], [28]. However, the differences between two-layer and three-layer skin models are not more than ~0.003 as the presence of semi-infinite fat layer in the three-layer skin model doesn't affect the reflectance calculations since the penetration depth of the MMW in the palm of hand skin is reported to be (1.2-0.65) mm [20], [28]. This penetration is less than the thickness of epidermis plus dermis layer 1.85 mm [20], [28], [33]. In addition, the fat layer of the skin contains large amount of water that attenuates the MMW [20]. As a result of low penetration depth and attenuation, the fat layer in the three-layer model of the skin doesn't cause significant difference in the reflectance calculations. Therefore, the results obtained from two and three-layers models are not dissimilar and this makes the two-layer model of the skin is sufficient for modelling the reflectance of palm of hand skin.
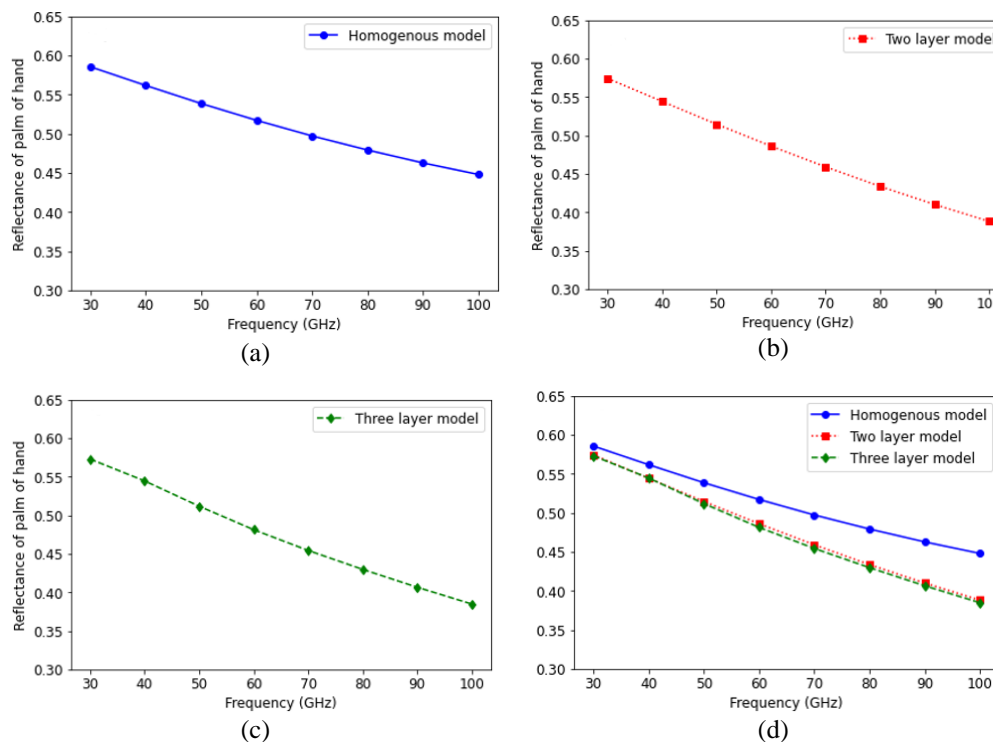

Figure 6. Reflectance of palm of hand skin using; (a) homogenous model, (b) two-layer model, (c) three-layer model, and (d) the results obtained from the three models are compared with each other's

3.2. Reflectance of forearm

This section presents the reflectance of the forearm skin obtained from the three models described in section 2. The reflectance of forearm skin is calculated in the frequency band 30-100 GHz using three models of the skin as illustrated in Figure 7. Homogenous skin model as in Figure 7(a), two-layer skin model as in Figure 7(b), and three-layer skin model as in Figure 7(c). The simulation results in Figure 7(a) show the variation in the reflectance of forearm skin over the MMW frequency band 30-100 GHz. The reflectance of forearm skin was found to be varied in the range of 0.61 (at 30 GHz) to 0.47 (at 100 GHz). The results obtained from three models are consistent as illustrated in Figure 7(d). The differences in the reflectance between homogenous and multilayer skin models was found to be not more than 0.014. The presence of thin SC layer and semi-infinite fat layer in the three-layer of forearm skin model doesn't affect the reflectance calculations of the forearm skin. This is due to the penetration depth of the MMW in the forearm skin that is reported to be 0.8 mm to 0.35 mm in the band (30-100) GHz [23]. This penetration is less than the thickness of the epidermis plus dermis layer of the forearm skin that is reported to be 1.45 mm [20], [28]. As a result of low penetration depth; the interaction of the MMW with the fat layer is very limited and it can be neglected since most of the MMW radiation is attenuated close to the skin surface [8]. Therefore, homogenous unilayer skin model is found to be sufficient for modelling the reflectance of forearm skin.
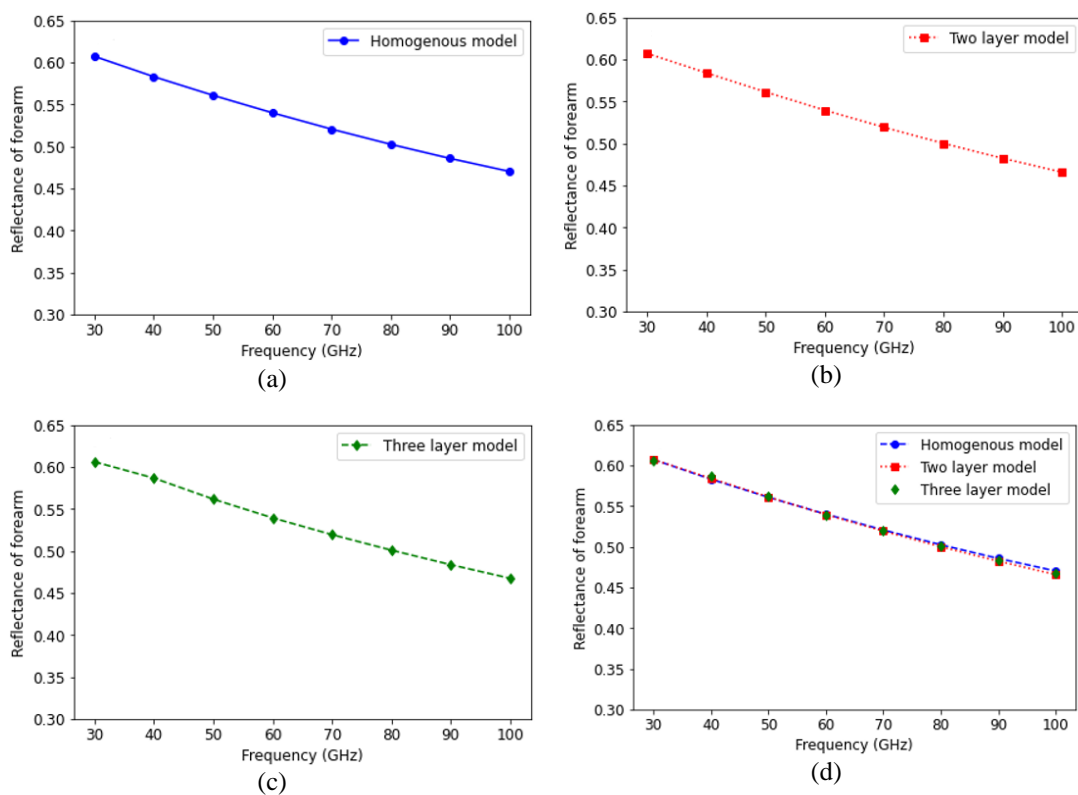

Figure 7. Reflectance of the forearm skin using; (a) homogenous skin model, (b) two-layer skin model, (c) three-layer skin model, and (d) the results obtained from the three models are compared with each other's

3.3. Models validiation

The reflectance calculations from the proposed models were compared with experimental measurements from the literature review. Table 3 shows a comparison in reflectance between two-layer palm of hand skin model and experimental measurements in [18], [20], [28]. The comparison in Table 3 indicates that reflectance calculation from two-layer model of the palm of the hand is very closed to that obtained from the experimental measurements in the literature. This indicates that the two-layer model gives an accurate estimation of the reflectance of the palm of hand skin.

Table 4 shows a comparison in reflectance between homogenous forearm skin model and experimental measurements in [18], [20], [28]. The comparison in Table 4 indicates that reflectance calculation from homogenous model is very closed to that obtained from the measurements in the literature review. This indicates that the homogenous model can provide precise estimation of the reflectance of the forearm skin.

Table 3. Reflectance comparison for palm of hand skin from two-layer model proposed in this paper and experimental measurements performed in literature

Frequency (GHz)	Palm of hand multilayer models	Palm of hand measurements	References
30	0.574	0.565	[20], [28]
40	0.554	0.547	[20], [28]
50	0.515	0.516	[20], [28]
60	0.486	0.484	[20], [28]
70	0.459	0.456	[20], [28]
80	0.434	0.435	[18]
90	0.410	0.412	[18]
100	0.388	0.385	[18]

Table 4. Reflectance comparison for forearm skin from homogenous model proposed in this paper and experimental measurements performed in literature

Frequency (GHz)	Forearm homogenous model	Forearm measurements	References
30	0.603	0.601	[20], [28]
40	0.583	0.577	[20], [28]
50	0.561	0.562	[20], [28]
60	0.540	0.535	[20], [28]
70	0.520	0.518	[20], [28]
80	0.503	0.502	[18]
90	0.486	0.484	[18]
100	0.470	0.470	[18]

3.4. Featured application: non-invasive diagnosis of skin diseases

In this research, the dielectric permittivity of healthy and diseased skin that measured in literature [34] were used to estimate the reflectance of healthy and diseased skin using homogenous skin model of forearm skin as illustrated in Figure 8 (for dry and healthy skin) and Figure 9 (for healthy skin and skin with malignant lesions). The models proposed in this research provide us with the reflectance values of the skin over a wide range of frequencies (30-100 GHz) for healthy and diseased skin. These values will help us to determine a threshold of healthy skin reflectance values over a wide range of frequency bands so, any deviations from this threshold can be identified as either high or low levels of the reflectance values. The main advantage of relying on reflectance as a quantity for assessing the skin conditions is that it can be measured using a non-contact sensor (radiometry) whereas the dielectric permittivity of the skin requires a coaxial probe in direct contact with the skin and this makes the probe not suitable to be used in the cases of diseased skin as it is painful and not comfortable to a patient suffering from skin conditions or diseases such as burn and malignancy.

Simulation results of the reflectance in Figure 8 indicate that there is 0.023 difference in reflectance values between healthy skin and dry skin over the frequency band from 30 GHz to 100 GHz. Dry skin here means any skin having lower water content due to age, eczema or psoriasis. These findings are in a good agreement with the reflectance measurements at 90 GHz [23]. The model presented herein allows us to extract the reflectance over a wide range of frequencies rather than at a single frequency.
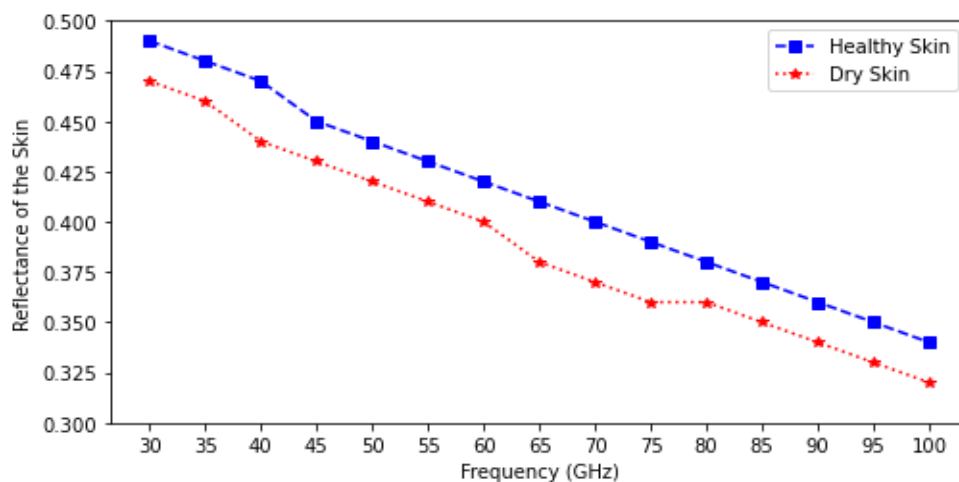

Figure 8. Reflectance calculation of dry and healthy skin over the frequency 30-100 GHz

Simulation results of the reflectance in Figure 9 indicate that there is 0.05 difference in reflectance values between healthy skin and skin with malignant lesions over the frequency band from 30 GHz to 100 GHz. These differences are due to variations in water content between healthy and diseased skin. These results agree with the reflectance measurements at the frequency of 90 GHz [23]. This indicates that the reflectance of the skin can be used for non-invasive diagnosis of skin diseases.
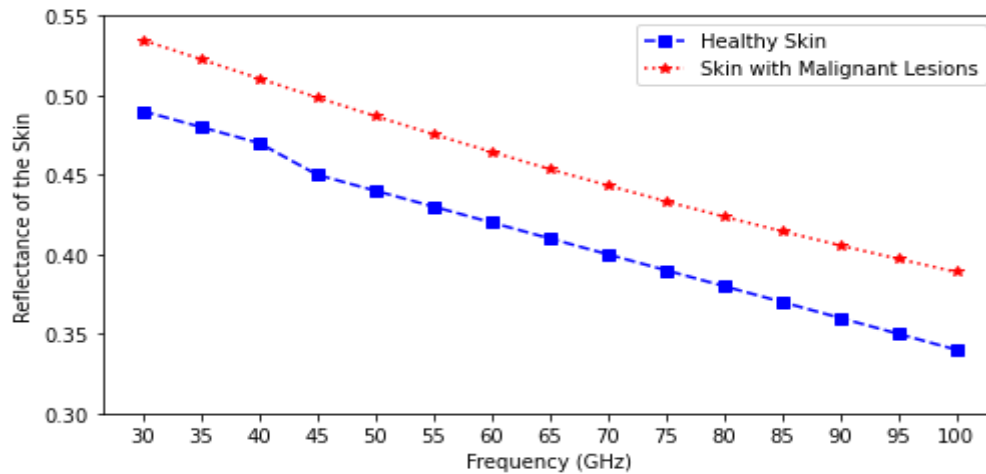

Figure 9. Reflectance calculation of skin with malignant lesions and healthy skin

4.   CONCLUSION

This paper proposes electromagnetics models for calculating the reflectance of the forearm and palm of hand skin. The reflectance of forearm skin was found to be varied in the range of 0.61 (at 30 GHz) to 0.47 (at 100 GHz), whereas it is in the range of 0.57 to 0.39 for the palm of the hand skin over the same frequency band. The importance of creating such a model for estimating skin reflectance across a wide range of MMW frequencies in which we can identify the range of reflectance across the human body. This will help in identifying abnormal reflectance values that will give indicators about the state of health of the human body as well as early detection of skin diseases. Moreover, MMW technology and devices are very expensive, and proposing skin models that can provide accurate calculations for human skin reflectance will be beneficial for healthcare professionals. For future work, it is recommended to collect more data and calculate the reflectance of the skin and then use these calculations to identify the threshold for healthy skin so any value that deviates from the norm will consider as an exceptional data point that indicates unhealthy skin.

REFERENCES

[1]   M. Zhadobov, N. Chahat, R. Sauleau, C. Le Quement, and Y. Le Drean, "Millimeter-wave interactions with the human body: State of knowledge and recent advances," *International Journal of Microwave and Wireless Technologies*, vol. 3, no. 2, pp. 237–247, Mar. 2011, doi: 10.1017/S1759078711000122.
[2]   O. P. Gandhi and A. Riazi, "Absorption of millimeter waves by human beings and its biological implications," *IEEE Transactions on Microwave Theory and Techniques*, vol. MTT-34, no. 2, pp. 228–235, Feb. 1986, doi: 10.1109/tmtt.1986.1133316.
[3]   P. F. M. Smulders, "Analysis of human skin tissue by millimeter-wave reflectometry," *Skin Research and Technology*, vol. 19, no. 1, Jun. 2013, doi: 10.1111/j.1600-0846.2012.00629.x.
[4]   O. Boric-Lubecke, Y. Nikawa, W. Snyder, J. Lin, and K. Mizuno, "Novel microwave and millimeter-wave biomedical applications," in *4th International Conference on Telecommunications in Modern Satellite, Cable and Broadcasting Services, ITELSIKS 1999 - Proceedings*, 1999, vol. 1, pp. 186–193, doi: 10.1109/TELSKS.1999.804724.
[5]   C. M. Alabaster, "Permittivity of human skin in millimetre wave band," *Electronics Letters*, vol. 39, no. 21, pp. 1521–1522, 2003, doi: 10.1049/el:20030967.
[6]   R. Appleby and R. N. Anderton, "Millimeter-wave and submillimeter-wave imaging for security and surveillance," *Proceedings of the IEEE*, vol. 95, no. 8, pp. 1683–1690, Aug. 2007, doi: 10.1109/JPROC.2007.898832.

[7] T. Wu, T. S. Rappaport, and C. M. Collins, "The human body and millimeter-wave wireless communication systems: Interactions and implications," in *IEEE International Conference on Communications*, Jun. 2015, vol. 2015-September, pp. 2423–2429, doi: 10.1109/ICC.2015.7248688.

[8] S. W. Harmer, S. Shylo, M. Shah, N. J. Bowring, and A. Y. Owda, "On the feasibility of assessing burn wound healing without removal of dressings using radiometric millimetre-wave sensing," *Progress In Electromagnetics Research M*, vol. 45, pp. 173–183, 2016, doi: 10.2528/PIERM15110503.

[9] A. Y. Owda, N. Salmon, and N. D. Rezgui, "Electromagnetic signatures of human skin in the millimeter wave band 80-100 GHz," *Progress In Electromagnetics Research B*, vol. 80, pp. 79–99, 2018, doi: 10.2528/PIERB17120403.

[10] D. M. Sheen, D. L. McMakin, and T. E. Hall, "Three-dimensional millimeter-wave imaging for concealed weapon detection," *IEEE Transactions on Microwave Theory and Techniques*, vol. 49, no. 9, pp. 1581–1592, 2001, doi: 10.1109/22.942570.

[11] H. Essen *et al.*, "Monitoring of wound healing by millimetre wave imaging," *in 35th International Conference on Infrared, Millimeter, and Terahertz Waves,* Sep. 2010, doi: 10.1109/ICIMW.2010.5612311.

[12] A. Y. Owda, "Passive millimeter-wave imaging for burns diagnostics under dressing materials," *Sensors*, vol. 22, no. 7, p. 2428, Mar. 2022, doi: 10.3390/s22072428.

[13] Q. Cassar *et al.*, "Association of the terahertz refractive index and morphological dilation operations for breast carcinoma detection," in *International Conference on Infrared, Millimeter, and Terahertz Waves, IRMMW-THz*, Aug. 2021, vol. 2021-August, doi: 10.1109/IRMMW-THz50926.2021.9567087.

[14] S. Kharkovsky, M. T. Ghasr, M. A. Abou-Khousa, and R. Zoughi, "Near-field microwave and mm-Wave noninvasive diagnosis of human skin," in *2009 IEEE International Workshop on Medical Measurements and Applications, MeMeA 2009*, May 2009, pp. 5–7, doi: 10.1109/MEMEA.2009.5167943.

[15] R. Aminzadeh, M. Saviz, and A. A. Shishegar, "Dielectric properties estimation of normal and malignant skin tissues at millimeter-wave frequencies using effective medium theory," in *22nd Iranian Conference on Electrical Engineering, ICEE 2014*, May 2014, pp. 1657–1661, doi: 10.1109/IranianCEE.2014.6999804.

[16] S. Gabriel, R. W. Lau, and C. Gabriel, "The dielectric properties of biological tissues: II. Measurements in the frequency range 10 Hz to 20 GHz," *Physics in Medicine and Biology*, vol. 41, no. 11, pp. 2251–2269, Nov. 1996, doi: 10.1088/0031-9155/41/11/002.

[17] A. Y. Owda and N. Salmon, "Variation in the electromagnetic signatures of the human skin with physical activity and hydration level of the skin," in *Millimetre Wave and Terahertz Sensors and Technology {XII}*, Oct. 2019, p. 1, doi: 10.1117/12.2533162.

[18] A. Y. Owda, N. Salmon, A. J. Casson, and M. Owda, "The reflectance of human skin in the millimeter-wave band," *Sensors (Switzerland)*, vol. 20, no. 5, p. 1480, Mar. 2020, doi: 10.3390/s20051480.

[19] V. P. Wallace *et al.*, "Terahertz pulsed imaging of basal cell carcinoma ex vivo and in vivo," *British Journal of Dermatology*, vol. 151, no. 2, pp. 424–432, Aug. 2004, doi: 10.1111/j.1365-2133.2004.06129.x.

[20] S. I. Alekseev and M. C. Ziskin, "Human skin permittivity determined by millimeter wave reflection measurements," *Bioelectromagnetics*, vol. 28, no. 5, pp. 331–339, Apr. 2007, doi: 10.1002/bem.20308.

[21] Y. Gao and R. Zoughi, "Millimeter wave reflectometry and imaging for noninvasive diagnosis of skin burn injuries," *IEEE Transactions on Instrumentation and Measurement*, vol. 66, no. 1, pp. 77–84, Jan. 2017, doi: 10.1109/TIM.2016.2620778.

[22] H. Hwang, J. Yim, J. W. Cho, C. Cheon, and Y. Kwon, "110 GHz broadband measurement of permittivity on human epidermis using 1 mm coaxial probe," in *IEEE MTT-S International Microwave Symposium Digest*, 2003, vol. 1, pp. 399–402, doi: 10.1109/mwsym.2003.1210961.

[23] A. Y. Owda and M. Owda, "Early detection of skin disorders and diseases using radiometry," *Diagnostics*, vol. 12, no. 9, p. 2117, Aug. 2022, doi: 10.3390/diagnostics12092117.

[24] Z. Vilagosh, A. Lajevardipour, and A. W. Wood, "Computational absorption and reflection studies of normal human skin at 0.45 THz," *Biomedical Optics Express*, vol. 11, no. 1, p. 417, Dec. 2020, doi: 10.1364/boe.377424.

[25] K. Das, T. Yuasa, T. Maeda, I. Nishidate, H. Funamizu, and Y. Aizu, "Simple detection of absorption change in skin tissue using simulated spectral reflectance database," *Measurement: Journal of the International Measurement Confederation*, vol. 182, p. 109684, Sep. 2021, doi: 10.1016/j.measurement.2021.109684.

[26] K. Li and K. Sasaki, "Monte carlo simulation of clothed skin exposure to electromagnetic field with oblique incidence angles at 60 GHz," *Frontiers in Public Health*, vol. 10, Feb. 2022, doi: 10.3389/fpubh.2022.795414.

[27] J. Wang, H. Lindley-Hatcher, X. Chen, and E. Pickwell-Macpherson, "Thz sensing of human skin: A review of skin modeling approaches," *Sensors*, vol. 21, no. 11, p. 3624, May 2021, doi: 10.3390/s21113624.

[28] S. I. Alekseev, A. A. Radzievsky, M. K. Logani, and M. C. Ziskin, "Millimeter wave dosimetry of human skin," *Bioelectromagnetics*, vol. 29, no. 1, pp. 65–70, Oct. 2008, doi: 10.1002/bem.20363.

[29] N. Chahat, M. Zhadobov, R. Augustine, and R. Sauleau, "Human skin permittivity models for millimetre-wave range," *Electronics Letters*, vol. 47, no. 7, pp. 427–428, 2011, doi: 10.1049/el.2011.0349.

[30] D. K. Ghodgaonkar, O. P. Gandhi, and M. F. Iskander, "Complex permittivity of human skin in vivo in the frequency band 26.5-60 GHz," in *IEEE Antennas and Propagation Society, AP-S International Symposium (Digest)*, 2000, vol. 2, pp. 1100–1103, doi: 10.1109/aps.2000.875414.

[31] S. Gabriel, R. W. Lau, and C. Gabriel, "The dielectric properties of biological tissues: III. Parametric models for the dielectric spectrum of tissues," *Physics in Medicine and Biology*, vol. 41, no. 11, pp. 2271–2293, Nov. 1996, doi: 10.1088/0031-9155/41/11/003.

[32] K. S. Cole and R. H. Cole, "Dispersion and absorption in dielectrics I. Alternating current characteristics," *The Journal of Chemical Physics*, vol. 9, no. 4, pp. 341–351, Apr. 1941, doi: 10.1063/1.1750906.

[33] N. Dagli, R. Dagli, and L. Thangavelu, "Interaction of millimetre waves used in 5G network with cells and tissues of head-and-neck region: A literature review," *Advances in Human Biology*, vol. 13, no. 2, p. 168, 2023, doi: 10.4103/aihb.aihb_133_22.

[34] D. Dancila *et al.*, "Millimeter wave silicon micromachined waveguide probe as an aid for skin diagnosis - results of measurements on phantom material with varied water content," *Skin Research and Technology*, vol. 20, no. 1, pp. 116–123, Jul. 2014, doi: 10.1111/srt.12093.

BIOGRAPHIES OF AUTHORS

Amani Yousef Owda 🆔 Ⓖ SC ↻ Assistant Professor in Computer Engineering and Data Science in the Faculty of Graduate Studies at the Arab American University in Palestine. She worked as a head of department of Natural, Engineering, and Technology Sciences in the Faculty of Graduate Studies at Arab American University from 2022 -2023. She worked as a research associate in the Faculty of Engineering at the University of Manchester from 2019 - 2020. In addition, she worked in the School of Engineering at Manchester Metropolitan University from 2015 – 2019. She worked at Birzeit University from 2007- 2011. She received her MSc. degree (Hons.) from The University of Manchester, UK in 2013, and her Ph.D. degree in Computer Engineering from Manchester Metropolitan University, UK in 2018. Since 2018, she leads research in multi-disciplinary fields with a focus on artificial intelligence, machine learning, decision support systems, image processing, medical applications of microwave and millimeter-wave imaging, security screening, and anomaly detection. She has published more than 43 articles in well reputable journals. She is a reviewer in many well-known Journals, and she is supervising MSc and PhD students. She can be contacted using the following emails: amani.owda@aaup.edu or amaniabubaha@gmail.com.

Majdi Owda 🆔 Ⓖ SC ↻ Associate Professor in Computer Science and Dean of Faculty in Data Science at the Arab American University in Palestine. In addition, he is a UNESCO Chair for Data Science for Sustainable Development. Worked as a head of the Department of Natural, Engineering, and Technology Sciences in the Faculty of Graduate Studies at Arab American University from 2020 -2022. Worked in the School of Computing, Mathematics, and Digital Technology at Manchester Metropolitan University from 2009 to 2020. He gained a BSc in Computer Science from the Arab American University in 2004, and an MSc by research in Computer Science with distinction from Manchester Metropolitan University in 2005 and a Ph.D. in Computer Science in 2011. His main research interests are AI Techniques for Natural Language Interfaces to Relational Databases, Data Science, Conversational Informatics, Conversational Agents, Knowledge Trees, Knowledge Engineering, Planning, Information Extraction, AI Techniques for the Help of Society, Web/Data/Text Mining, Digital Forensics Processes and Frameworks, Digital Forensics Artefacts, Information Retrieval from Large Data Sources, Internet of Things Frameworks and Internet of Things Digital Forensics Artefacts and Security. He can be contacted using the following email: majdi.owda@aaup.edu.